Ecography

ECOG-05012
Testolin, R., Attorre, F. and Jiménez-Alfaro, B. 2020. Global distribution and bioclimatic characterization of alpine biomes. – Ecography doi: 10.1111/ecog.05012

Supplementary material

Appendix 1

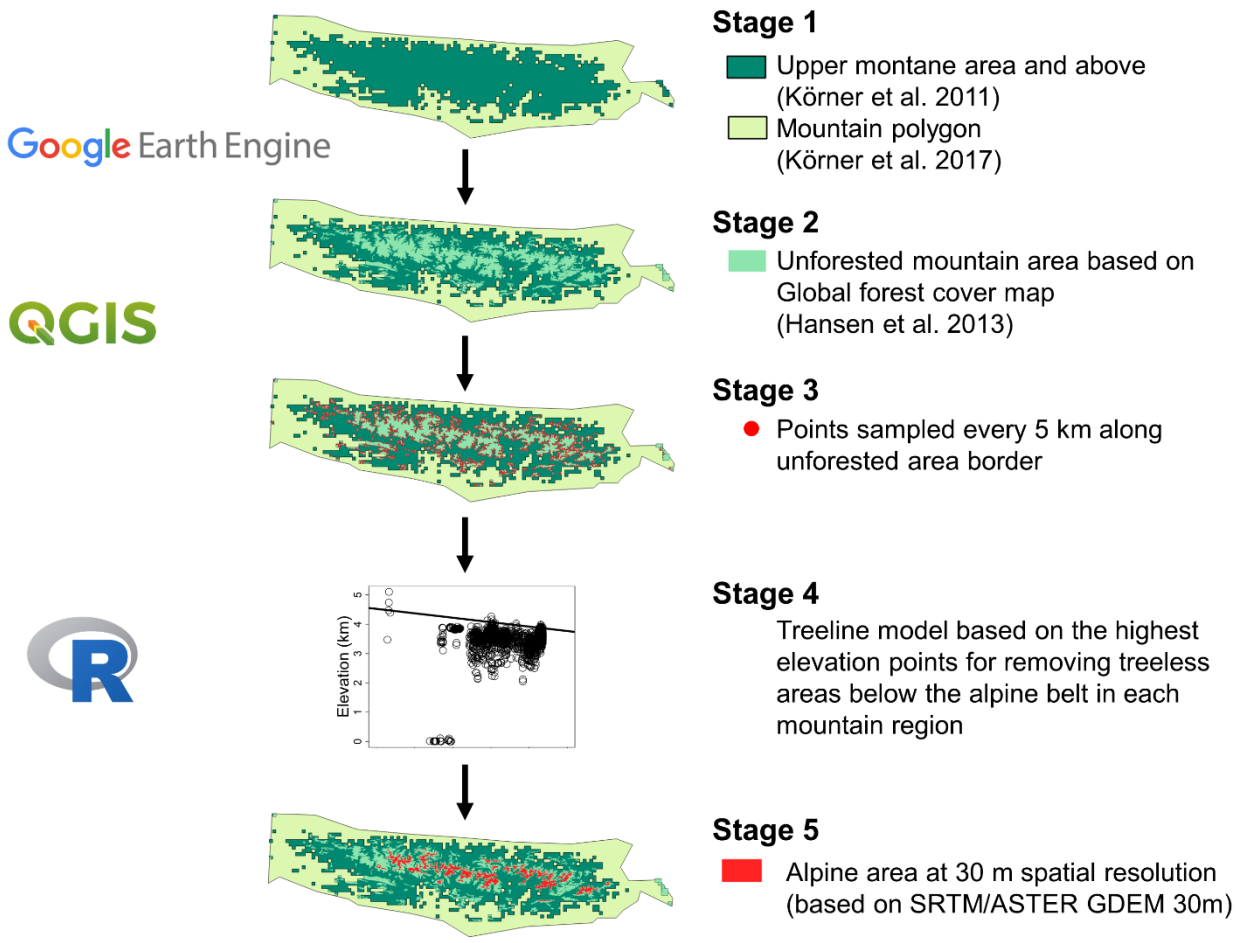

Figure A1. Schematic representation of the workflow for modeling the extent of alpine areas based on high-resolution forest cover and mountain inventory data exemplified for a single mountain region.

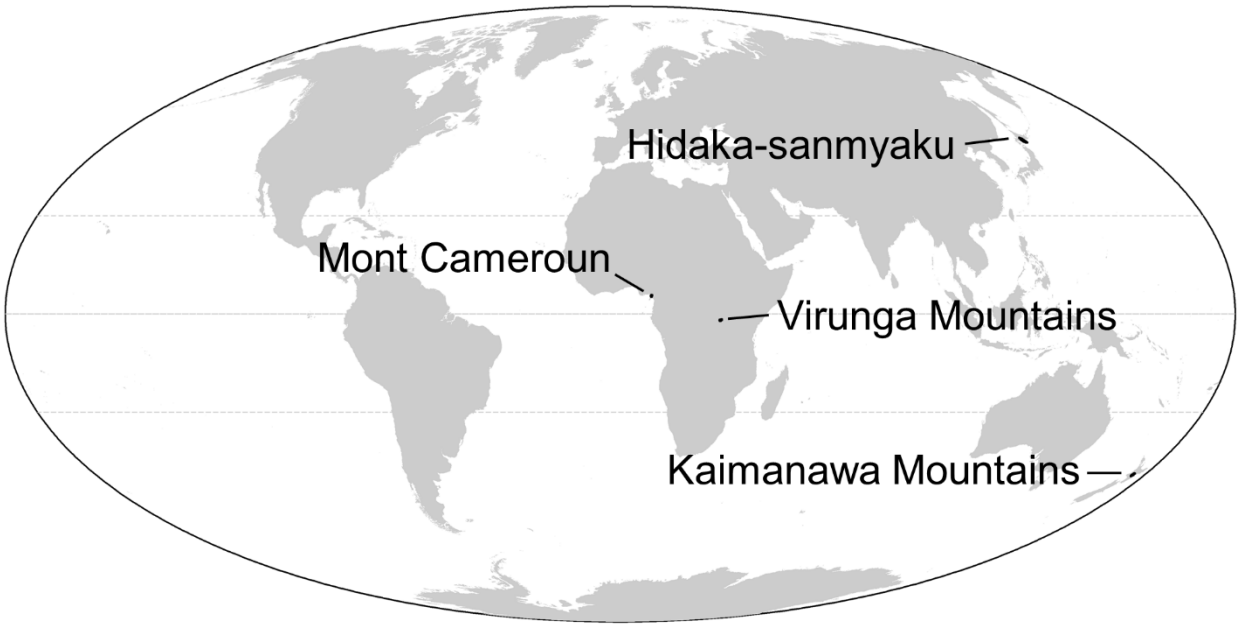

Figure A2. Distribution of mountain regions that, despite hosting an alpine belt, were excluded due to the spatial resolution of the present study.

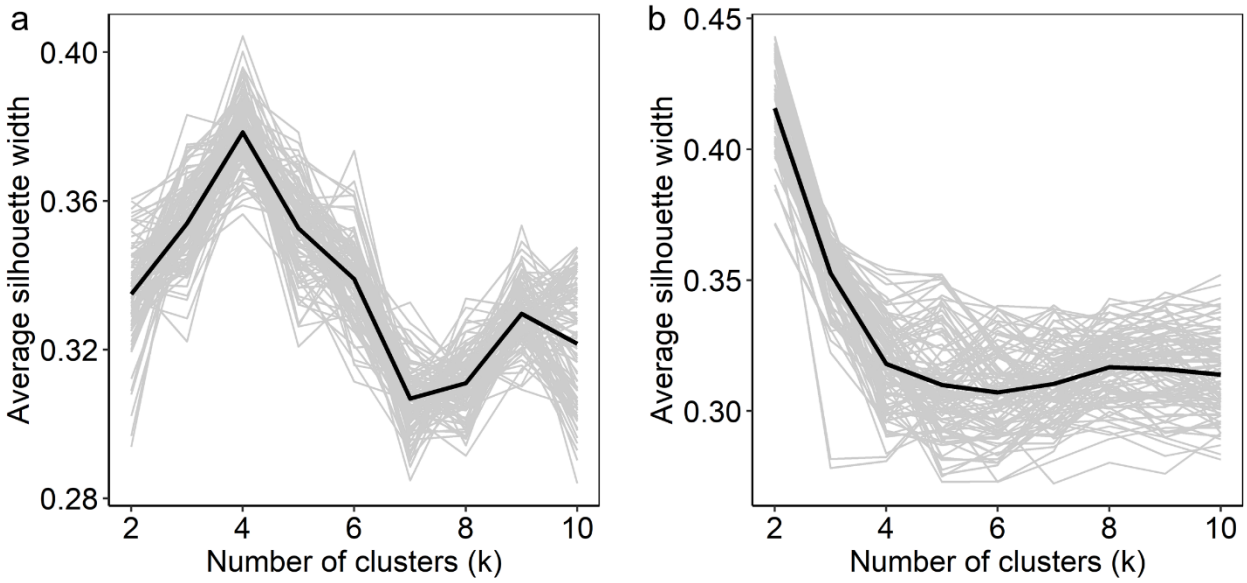

Figure A3. Average silhouette widths at different k for (a) the CLARA algorithm and (b) the hierarchical clustering with Ward2 method. The grey lines represent the average widths for each of the 100 random samples. The black line represents the mean of the average silhouette widths across all samples.

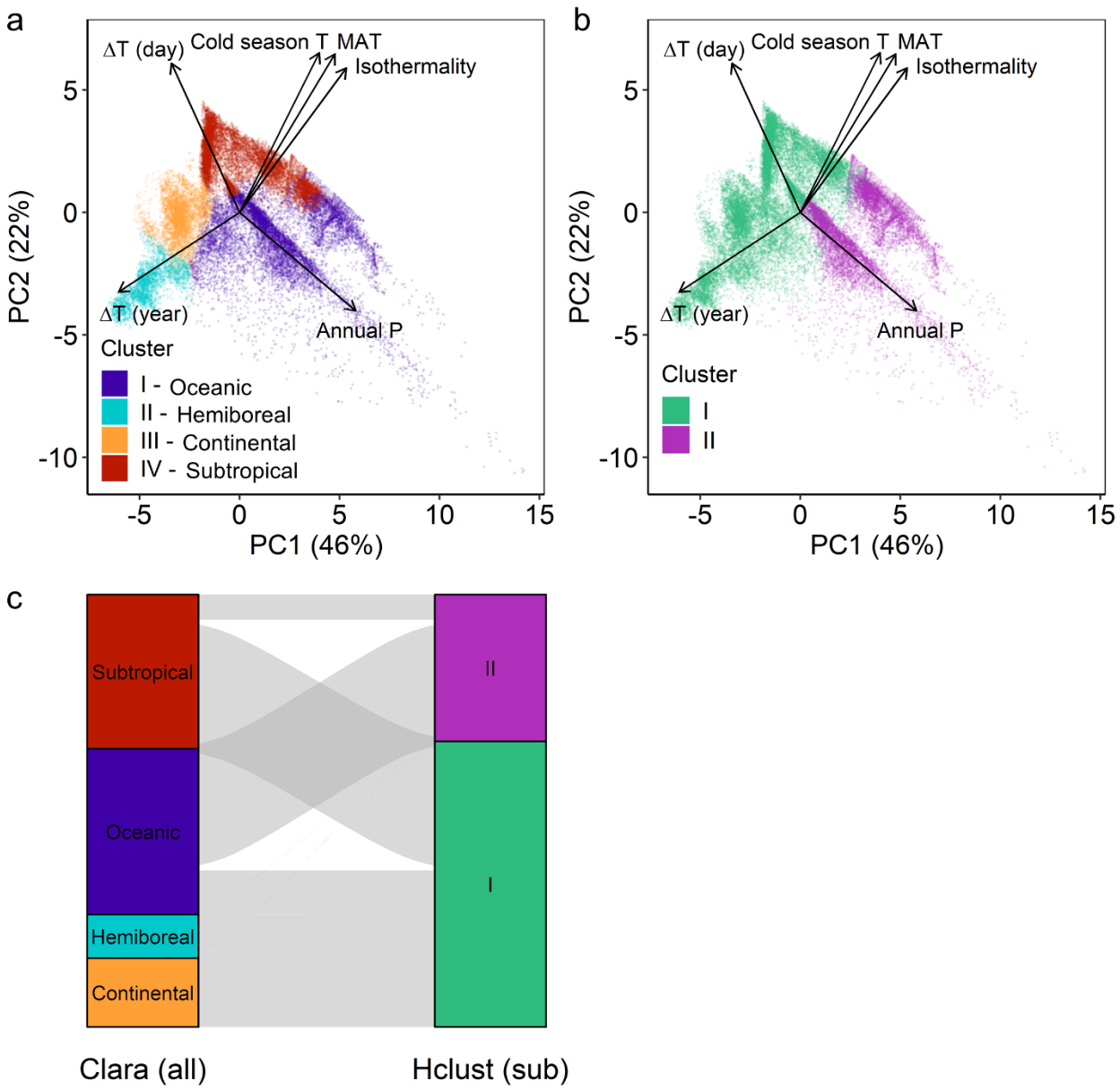

Figure A4. Comparison between the hierarchical clustering output of a subsample of 30,000 climatic records and the corresponding clusters defined by the CLARA algorithm at the same locations based on the whole data set. The top panel contains the biplots of the principal component analysis of 19 climatic variables. The arrows indicate the loadings of selected climatic variables (correlation > 0.3 with one of the two axes). Points are colored according to the clusters as defined by CLARA (a) and the hierarchical clustering (b). Variables names' abbreviations and symbols (MAT: Mean annual temperature, P: Precipitation, T: temperature, Δ: Difference). (c) Alluvial plot representing the correspondence between the two clustering algorithms on the subset. The panels are colored according to the clusters as reported in (a) and (b).

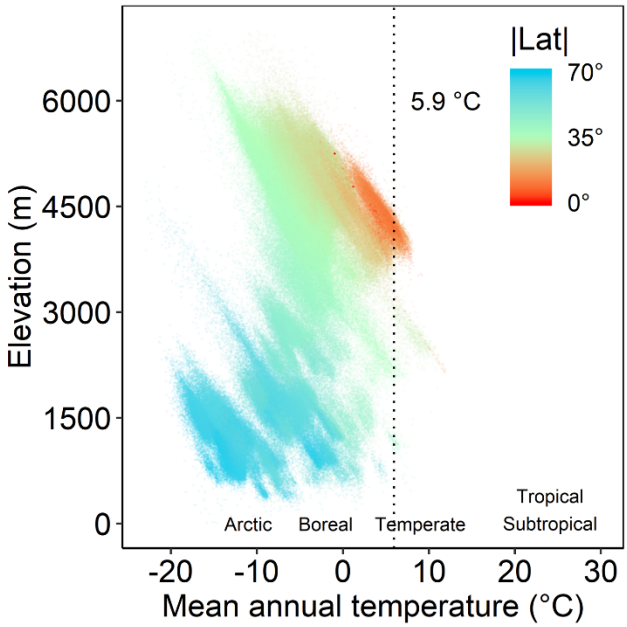

Figure A5. Elevation of alpine areas along the temperature gradient. The names at the bottom of the plot indicate major biomes according to Whittaker and are placed close to their mean temperature value. The dotted line represents the 99th percentile of the distribution of temperature values. To improve readability, the figure is based on a random subset of 500,000 30 arc-second cells in alpine areas. Points are colored according to their distance from the equator (|Lat|).

Table A1. List of mountain regions for which no or few points were available to model treeline elevation. The mountain regions whose model was used to estimate the former, as well as the model predictors are also provided.

Continent	Mountain ranges	Model	Predictors
Asia	Anyemaqen Shan	Himalaya	Northness + Latitude
	Chola Shan		
	Daban Shan		
	Danghe Nanshan		
	Datong Shan		
	Karakoram		
	Lenglong Ling		
	Ningjing Shan		
	Pamir Mountains		
	Qaidam Shan		
	Qinghai Nanshan		
	Shule Nanshan		
	Tanggula Shan		
	Tergun Daba Shan		
	Tibetan Plateau (Xizang Gaoyuan)		
	Tulai Nanshan		
	Tulai Shan		
	Yema Nanshan		
	Yema Shan		
	Zoulang Nanshan		
	Ferganskiy Khrebet	Khrebet Terskey Alatau	Northness
	Khrebet Kokshaal-Tau		
	Dahei Shan Karlik Shan	Bogda Shan	Northness
	Gichgeniyn Nuruu	Altai Mountains	Northness
	Hangayn Nuruu		
	Horh Uul		
	Agri Dagi	Kuzey Anadolu Daglari / Pontus Mountains	Northness
	Ala Daglari		
	Erciyas Dagi		
	Hakkari Daglari		
	Kuh haye Sabalan		
	Suphan Dagi		
	Eren Habirga Shan	Horo Shan	Northness
	Tien Shan-02	Tien Shan-01	Northness
South America	Altiplano		Northness

	Cordillera de los Frailes	Cordillera Oriental Peru Bolivia Chile + Cordillera Frontal	+ Latitude
	Central Volcanic Zone		
	Cerro de Ansilta		
	Cordillera de Lipez		
	Cordillera de Oliva		
	Cordillera de Ollita		
	Cordillera Domeyko		
	Cordillera Frontal		
	Cordillera Occidental Peru Bolivia Chile		
	Cordillera Oriental (Argentina)		
	Cordillera Oriental Peru Bolivia		
	Sierra de Famatina		
	Sierra de la Punilla		
	Sierra de Tatul		
	Sierra del Nevado		
	Sierra Fiambala		
	Sierra Tigre		
	Sierra Tontal		
	Sierra Ambato	Sierra del Alconquija	Northness
	Sierra de Velasco		